ASSESSMENT OF SHIELDING EFFECTIVENESS BY USING ELECTROMAGNETIC TOPOLOGY METHOD

A THESIS SUBMITTED TO
THE GRADUATE SCHOOL OF NATURAL AND APPLIED SCIENCES
OF
MIDDLE EAST TECHNICAL UNIVERSITY

BY

HALİL İBRAHİM YAŞLAK

IN PARTIAL FULFILLMENT OF THE REQUIREMENTS
FOR
THE DEGREE OF MASTER OF SCIENCE
IN
ELECTRICAL AND ELECTRONICS ENGINEERING

FABRUARY 2013

Approval of the thesis

ASSESSMENT OF SHIELDING EFFECTIVENESS BY USING ELECTROMAGNETIC TOPOLOGY METHOD

submitted by **HALİL İBRAHİM YAŞLAK** in partial fulfillment of the requirements for the degree of **Master of Science in Electrical and Electronics Engineering Department, Middle East Technical University** by,

Prof. Dr. Canan ÖZGEN _____
Dean, Graduate School of **Natural and Applied Sciences**

Prof. Dr. İsmet ERKMEN _____
Head of Department, **Electrical and Electronics Engineering**

Prof. Dr. Şimşek DEMİR _____
Supervisor, **Electrical and Electronics Eng. Dept., METU**

Examining Committee Members:

Prof. Dr. Gönül TURHAN SAYAN _____
Electrical and Electronics Engineering Dept., METU

Prof. Dr. Şimşek DEMİR _____
Electrical and Electronics Engineering Dept., METU

Prof. Dr. Gülbin DURAL _____
Electrical and Electronics Engineering Dept., METU

Prof. Dr. Özlem AYDIN ÇİVİ _____
Electrical and Electronics Engineering Dept., METU

Can BAYSEFEROĞULLARI, M. Sc. _____
MGEO, ASELSAN

Date: 01.02.2013

I hereby declare that all information in this document has been obtained and presented in accordance with academic rules and ethical conduct. I also declare that, as required by these rules and conduct, I have fully cited and referenced all material and results that are not original to this work.

Name, Last name : HALİL İBRAHİM YAŞLAK

Signature :

ABSTRACT

ASSESSMENT OF SHIELDING EFFECTIVENESS BY USING ELECTROMAGNETIC TOPOLOGY METHOD

YAŞLAK, Halil İbrahim
M.Sc., Department of Electrical and Electronics Engineering
Supervisor: Prof. Dr. Şimşek DEMİR

February 2013, 37 pages

In this thesis, determination of the shielding effectiveness of a rectangular shielding box with apertures on its walls by using electromagnetic topology (EMT) technique based on Baum-Liu-Tesche (BLT) equation is presented. The presented technique is applied to determine the field penetration into various rectangular shielding boxes with different sizes and aperture dimensions. An HP branded computer case is also analysed as a rectangular shielding box with a CD driver slot as an aperture. Results on electromagnetic field penetration through the apertures into the boxes at different frequencies are obtained by using the presented method and compared with the results obtained by using CST MICROWAVE STUDIO® software simulation.

Keywords: Shielding effectiveness, shielding box, apertures, electromagnetic compatibility, electromagnetic interference, electromagnetic topology, BLT equation.

ÖZ

EKRANLAMA ETKİNLİĞİNİN ELEKTROMANYETİK TOPOLOJİ YÖNTEMİ KULLANILARAK BELİRLENMESİ

YAŞLAK, Halil İbrahim
Yüksek Lisans, Elektrik Elektronik Mühendisliği Bölümü
Tez Yöneticisi: Prof. Dr. Şimşek DEMİR

Şubat 2013, 37 sayfa

Bu tezde, duvarlarında açıklıklar bulunan dikdörtgensel bir ekranlama kutusunun ekranlama etkinliğini Baum-Liu-Tesche (BLT) denklemine dayalı elektromanyetik topoloji yöntemi ile belirlenmesi sunulmuştur. Sunulan yöntem, değişik kutu ve açıklık boyutlarına sahip farklı dikdörtgensel ekranlama kutularına uygulanmıştır. Ayrıca bir HP marka bilgisayar kasası dikdörtgensel bir ekranlama kutusu olarak ve CD sürücüsü yuvası açıklık olarak ele alınarak incelenmiştir. Sunulan yöntem kullanılarak farklı frekanslarda elde edilen, açıklıklardan kutu içerisine nüfuz eden elektromanyetik alan sonuçları, CST MICROWAVE STUDIO® yazılımı kullanılarak elde edilen simülasyon sonuçları ile karşılaştırılmıştır.

Anahtar Kelimeler: Ekranlama etkinliği, ekranlama kutusu, açıklıklar, elektromanyetik uyumluluk, electromanyetik girişim, elektromanyetik topoloji, BLT denklemi

to my devoted wife

ACKNOWLEDGEMENTS

Before beginning; declaring sympathies and thankfulness to whom contributed this work is a great pleasure for me.

First and foremost, I would like to state gratefulness to my thesis supervisor Prof. Dr. Şimşek DEMİR who has maintained his support, knowledge and patience throughout the thesis study.

I also express my gratitude to my manager Mr. Yüksel SERDAR for letting and supporting of my thesis study.

I am grateful to ASELSAN for providing both financial and technical opportunities to complete this study.

I offer my best appreciation to my parents, Hüsamiye and Kemal YAŞLAK. They raised me, took care of me, taught me and support me.

Lastly, I would like to extend my special appreciation and gratitude to my wife Yeşim YAŞLAK for her endless support and encourages attitude which helped me think positively in any circumstances. To her, I dedicate this thesis.

TABLE OF CONTENTS

LIST OF TABLES

TABLES

LIST OF FIGURES

FIGURES

LIST OF ABBREVIATONS

EM	: Electromagnetic
EMI	: Electromagnetic Interference
EMC	: Electromagnetic Compatibility
BLT	: Baum-Liu-Tesche
EMT	: Electromagnetic Topology
CST	: Computer Simulation Technology
FIT	: Finite Integration Technique
BLC	: Branch-Line Coupler
FDTD	: Finite Difference Time Domain
FEM	: Finite Element Method
MoM	: Method of Moments
FIT	: Finite Integration Technique
PEC	: Perfect Electric Conductor
PCB	: Printed Circuit Board

CHAPTER 1

INTRODUCTION

Most of the modern electronic systems consist of different electronic units. These units may generate electromagnetic waves while operating. Electromagnetic waves generated inside an electronic system can affect itself or other systems outside. Electromagnetic interference (EMI) can be defined as the interference of an electromagnetic wave which causes a malfunction or a damage of the system generates it or another system outside [1]. Negative effects of EMI differ from failure of the anti-lock braking system of a mobile car to the failure of the flight control system of an aircraft. These examples show that EMI has a vital importance in our lives. Due to the importance of the issue, EMI has become one of the most important research topics in electronics. In 1995, NASA published a report about electromagnetic system failures and anomalies caused by EMI and case histories [2].

When EMI is the subject, first thing that comes to mind is shielding. Electromagnetic shielding can be defined as anything that used for the reduction of EM field in a prescribed region. In general, it is used to increase the EM immunity of electronic devices or systems against external electromagnetic fields. A shield is any enclosure that lowers the electromagnetic field inside the space enclosed [3].

In system level, to protect an electronic system from another one, shielding boxes are used. We can provide a full EMI protection to a system by putting it in a case made of a metal with high conductivity with no aperture however it is not possible since apertures are needed for various reasons such as input and output connections, visual access windows, ventilation openings, mounting holes and etc. In most situations, leakage of the electromagnetic energy from a metallic enclosure depends not the physical characteristics of the metal but size, shape and location of the apertures [4].

In addition to the protection of the electronic systems from unwanted electromagnetic field penetrations that may cause malfunction or damage, shielding and shielding enclosures are also the subject of Tempest applications. The objective of Tempest shielding is blocking the escape of electromagnetic radiation (EMR) emitted from a computer or telecommunications device which can be used to extract information. One of the methods that is used for this purpose is putting the equipment emitting EMR in a room or building which behaves as a shielding box. Windows, doors and any other interface between the room/building and outside are exactly the apertures on the shielding box.

There are many numerical and analytical methods for analysing EM interaction phenomenon into an electronic system [5]. The numerical methods include the finite difference time domain (FDTD) method [6] , the method of moment (MoM) [7], the finite element method (FEM) [8] and transmission line modelling [9]. In analytical methods, electric and magnetic field interference of a cavity with aperture explored by using circuit

equivalent approach [3], [10], [11]. Numerical methods are relatively accurate but long computation time, detailed mesh generation and large amounts of data are needed. On the other hand, analytical methods require short computation times, but use various assumptions which cause validity problem at high frequencies [12].

The Electromagnetic Topology (EMT) was first introduced by Baum and Tesche in 1970's as a simulation approach to analyze EMI phenomenon based on transmission-line theory [13], [14]. EMT divides a complex system into smaller sub-volumes and constructs a network from these sub-volumes consisting of nodes and tubes like a transmission-line network. After characterizing the scattering and propagation parameters of the nodes and tubes and then obtaining scattering and propagation supermatrices, it reconstructs the whole system by using Baum-Liu-Tesche (BLT) equation which was introduced in [15] for the first time for multiconductor transmission-line networks by Baum, Liu and Tesche. Most important advantage of the method is its fast computation time since the scattering parameters of sub-volumes can be determined by using data sheets, using simulation tools or experimental results. After obtaining supermatrices by means of these type of methods, BLT equation computes the fields of the system in only one calculation step [1].

In this thesis, electromagnetic topology (EMT) method based on BLT equation is used for the analysis of EM interference from an external field into rectangular shielding boxes through a rectangular aperture on their front faces and shielding effectiveness (SE) of the boxes are assessed. A plane wave is used as external field source and the electric field intensities in the shielding boxes are computed. Three different boxes are analyzed which have different dimensions and different aperture sizes. Same boxes are also examined in CST MICROWAVE STUDIO® simulation software which uses a 3-D simulation technique based on the finite integration technique (FIT). Results of the proposed method are compared with the simulation results.

The remaining parts of the thesis are organized as follows:

In Chapter 2, a literature survey about the basics of the subject, previous and current methods used for the assessment of SE of shielding boxes and the origins of the EMT method and BLT equation is presented.

In Chapter 3, a simple Branch-Line Coupler (BLC) is analyzed and its output voltages are calculated by BLT equation in order to examine and understand the BLT equation.

In Chapter 4, a computer case with a CD Driver aperture is analyzed by BLT equation based on EMT and CST MICROWAVE STUDIO® simulation results are introduced. At the end of the chapter, results of both methods are compared.

In Chapter 5, conclusions from this work are drawn and works that can be carried out in the future are stated.

CHAPTER 2

LITERATURE SURVEY

2.1 EM Shielding

Electromagnetic waves generated inside an electronic system can affect itself or other systems outside. Electromagnetic interference (EMI) can be defined as the interference of an electromagnetic wave which causes a malfunction or a damage of the system generates it or another system outside [1]. Since modern electronic systems are very complicated and susceptible to electromagnetic interference, EMI is one of the most important problems in electronics. Electromagnetic shielding can be defined as anything that used for the reduction of EM field in a prescribed region. In general, it is used to increase the EM immunity of the electronic devices or systems against external electromagnetic fields. By doing so, improvement of the electromagnetic compatibility (EMC), which is defined as the capability of operation of the electronic devices or systems in the intended electromagnetic environment at an efficient level, can be achieved. Electromagnetic shielding is used also for data security in telecommunications [16] and Tempest applications.

2.2 Shielding Boxes

A shield simply defined as any enclosure that is used to lower the electromagnetic field inside the space enclosed [3]. A shielding box is a metallic enclosure which consists of an empty cavity with metallic walls [16]. In literature, shielding boxes is also called as cavity and enclosure. For instance, while it is called as cavity in [1], [3], [11], [16] , and [18], it is called as enclosure in [4], [10], and [18–22].

In system level, to protect an electronic system from another one, shielding boxes are used. A full EMI protection for a system can be provided by putting it in a high conductive metallic box with no aperture however it is not possible since apertures are needed for various reasons such as input and output connections, visual access windows, ventilation openings, mounting holes and etc. Such electromagnetic coupling paths worsen the shielding performance [21]. In most cases, leakage of the electromagnetic energy from a metallic enclosure depends not the physical characteristics of the metal but size, shape and location of the apertures [4].

2.3 Shielding Effectiveness

In the general sense, the shielding effectiveness (SE) is a measure of EM field reduction at a given point in space after insertion of a shield between the reference EM field source and that point [16]. It is an important parameter for an electronic system since it affects the electromagnetic compatibility of the system [23].

The shielding effectiveness (SE) is defined as the ratio of the field strengths, usually expressed in decibels, in the presence and absence of the shielding enclosure [15]. For a given point in the shielding enclosure, an electric shielding effectiveness SE_E and a magnetic shielding effectiveness SE_M can be defined [10]. The electric shielding effectiveness is expressed as

$$SE_E = -20\log\left(\frac{\left|\vec{E}_{\text{int}}\right|}{\left|\vec{E}_{\text{ext}}\right|}\right) \tag{2.1}$$

and the magnetic shielding effectiveness is expressed as

$$SE_M = -20\log\left(\frac{\left|\vec{H}_{\text{int}}\right|}{\left|\vec{H}_{\text{ext}}\right|}\right) \tag{2.2}$$

where $\vec{E}_{\text{int}}$ is the electric field at the point inside the shielding enclosure and $\vec{E}_{\text{ext}}$ is the electric field at the same point in absence of the shielding enclosure [5]. Similarly, $\vec{H}_{\text{int}}$ is the magnetic field at the point inside the shielding enclosure and $\vec{H}_{\text{ext}}$ is the magnetic field at the same point in absence of the shielding enclosure.

Note that, the shielding ability of a shielding box is characterized by its shielding effectiveness and the SE of a practical shielding box is determined mainly by its apertures [23].

2.4 Analysis Methods for Shielding Effectiveness

Starting point of the analysis of any electromagnetic problem is the Maxwell's equations [16]. However, their solutions are very complex and generally not practical for real problems. Therefore, numerical or analytical modeling is required in order to solve the real EM problems. Since the assessment of the shielding effectiveness of a shielding box is also a real EM problem, several methods have been developed to solve the problem. These methods can be classified in two main groups as *numerical* and *analytical* methods.

2.4.1 Numerical Methods

Numerical methods used for the analysis of shielding effectiveness are based on Maxwell's equations just like every EM problems. They require a numerical modeling of the problem and a digital computer to get numerical results. Numerical methods that are used in the literature for the analysis of shielding effectiveness of a shielding box include the finite difference time domain (FDTD) method [6], the method of moment (MoM) [7], the finite element method (FEM) [8] and transmission line modeling [9]. These methods carry out the solutions in the time or frequency domain.

Computer simulation tools also solve the electromagnetic problems by using certain numerical techniques. The tool that is used in this thesis, CST MICROWAVE STUDIO®, is based on the finite integration technique (FIT) and analyzes the shielding effectiveness of the shielding boxes with this method in the time domain.

For the analysis of the SE of shielding boxes, numerical methods give relatively accurate results. On the other side, long computation time, detailed mesh generation and large amount of data are needed [12] for the analysis of shielding boxes which contains some

electronic parts such as printed circuit boards (PCBs), cables, and etc. and have different apertures on their walls. This is the Achilles' heel of the numerical methods for shielding effectiveness analysis of the complex shielding boxes.

2.4.2 Analytical Methods

SE of shielding boxes are analyzed also by various analytical methods in the literature. Many of the analytical formulations are derived from the Bethe's theory of diffraction through holes [24], and applied only to electrically small apertures [22]. One part of the analytical methods is derived from a power-balance method and the Ott's equation $S_E = 20\log_{10}\lambda/2l$ [25], where λ is the wavelength in free-space and l is the longest dimension of the aperture [10].

The third type of the analytical modeling of the shielding boxes with apertures are based on the circuit equivalence modeling of the box and apertures [3], [10], [11]. In the equivalent circuit, the shielding box is modeled as a shorted waveguide and the aperture is modeled as a coplanar strip transmission line shorted at each end.

Analytical methods based on Bethe's theory can be applied only on electrically small apertures and they cannot be used for electrically large apertures. Methods based on Ott's equation assume that the SE depends only on the wavelength and the longest dimension of the aperture, however it is experimentally found that SE depends also on the dimensions of the shielding box and the point at which SE is measured [23]. Besides, some methods based on the circuit equivalence modeling applies only below the cutoff frequency of the cavity(box) [4] and validity of some others may be questionable at high frequencies since they are based on several assumptions to simplify the problem [5].

Electromagnetic topology method based on the BLT Equation is also an analytical method and it is presented as a separate main heading since it is the main topic of this thesis.

2.5 Electromagnetic Topology based on BLT Equation

2.5.1 Electromagnetic Topology

The Electromagnetic Topology (EMT) was first introduced by Baum and Tesche in 1970's as a simulation approach to analyze EMI phenomenon based on transmission-line theory [13], [14]. EMT is a helpful technique to solve electromagnetic compatibility (EMC) problems of complicated electronic systems. It is difficult to analyze the electrically large systems due to their complexity and several ways of interaction of EM fields into the system some of which can be written as:

- Capacitive and inductive coupling,
- Direct EM field coupling within the system,
- EM field penetration through apertures,
- Diffusive penetrations through imperfect shielding conductors,
- Cavity-mode resonances.

Figure 2.1 shows an example of electrical system illuminated by an external source [26]. As it is seen on the example, even on the main case of the system there are many apertures that are mandatory for the proper operation of the system.

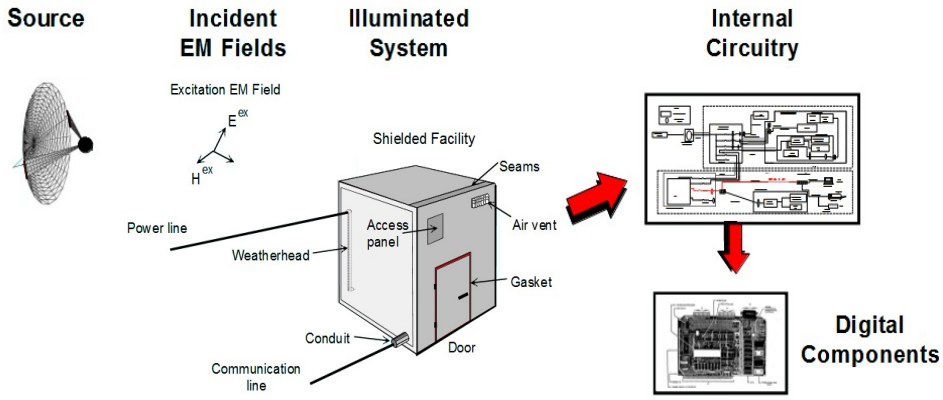

Figure 2.1 Example of an electrical system illuminated by an external source

Since there are too many penetration and coupling points on an electrical system it is difficult to analyze such a system. EMT eases the analysis of such systems by a three-step analysis:

1. Division of the structure of the main system into a set of sub-volumes
2. Characterization of those sub-volumes
3. Reconstruction of the main system by using BLT equation[1].

2.5.2 BLT Equation

The BLT equation is first proposed by Baum, Liu and Tesche in 70's for the analysis of multiconductor transmission line networks [15]. The conventional BLT equation describes the voltage and current wave propagation along transmission lines in a transmission line network [26]. BLT equation is a matrix equation which describes the voltages and/or currents at all of the junctions that interconnect the conductors in the network. It is similar to the node analysis in conventional circuit theory but the effects of EM propagation along the individual conductors are considered in the BLT equation.

Firstly, it is beneficial to review of the derivation of the conventional BLT equation and then introduce the extension of the BLT equation use for the analysis of the EM field interaction within a complex system.

As it is mentioned above, conventional BLT equation is used for the definition of voltage and current wave propagation in a transmission line network. Here, it is quite helpful to introduce the formulation of the equation for a single-line transmission line network in Figure 2.2 (a) instead of a complex one. This will show the overall formulation approach and it can be generalized for a multiconductor transmission line network. Note that this analysis is in the frequency domain and time dependence is assumed as $e^{j\omega t}$.

The network in Figure 2.2 is a two wire transmission line with a length of *L* and characteristic impedance of Z_c . It is assumed that propagation constant is γ . The transmission line is terminated at each end by the loads Z_{L1} and Z_{L2} . It is also

assumed that the network is excited by a current and voltage source, V_s and I_s, at $x = x_s$.

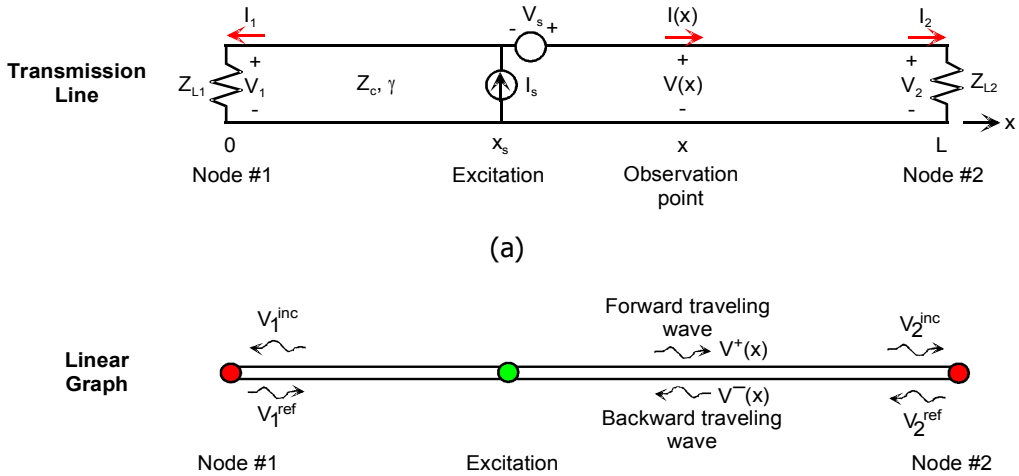

Figure 2.2 A single-line transmission line network (a) and its linear graph representation (b).

2.5.2.1 The Voltage BLT Equation

Derivation of the BLT equation can be achieved for either the load voltages or the load currents. Both of the derivations are based on the voltage responses. Notice that there are travelling voltage waves propagating in the direction V^+ and in the direction V^- as shown in the Figure 2.2 (b). Since these waves propagate on the transmission line with a $e^{\pm\gamma}$ term, at any position x on the line total voltage is calculated as the sum of the traveling waves propagating in positive and negative directions.

$$V(x) = V^+(x) + V^-(x) \qquad (2.3)$$

The propagation constant γ is equal to the $jk = j2\pi/c$, which is the lossless propagation constant in free-space.

As it is shown in Figure 2.2 (b), voltages waves can be described as *incident* and *reflected* voltage waves, V^{inc} and V^{ref}. So, we can write the positive and negative traveling voltage waves at the nodes as following:

$$V^+(0) \equiv V_1^+ = V_1^{ref} \;\; ; \;\; V^-(0) \equiv V_1^- = V_1^{inc} \quad \text{(at node 1)} \qquad (2.4a)$$

$$V^+(L) \equiv V_2^+ = V_2^{inc} \;\; ; \;\; V^-(L) \equiv V_2^- = V_1^{ref} \quad \text{(at node 2)} \qquad (2.4b)$$

The sources at $x = xs$ produce a positive traveling wave $V_s^+(x)$ for $x > x_s$ and a negative traveling wave $V_s^-(x)$ for $x < x_s$ as shown in Figure 2.3 . These voltage waves in terms of the sources can be written as

$$V_s^+(x)=\frac{1}{2}(V_s+Z_c I_s)e^{-\gamma(x-x_s)} \quad ; \quad V_s^-(x)=0 \quad \text{(for} \quad x>x_s \quad \text{)} \quad \text{(2.5a)}$$

$$V_s^-(x)=\frac{-1}{2}(V_s-Z_c I_s)e^{+\gamma(x-x_s)} \quad ; \quad V_s^+(x)=0 \quad \text{(for} \quad x<x_s \quad \text{)} \quad \text{(2.5b)}$$

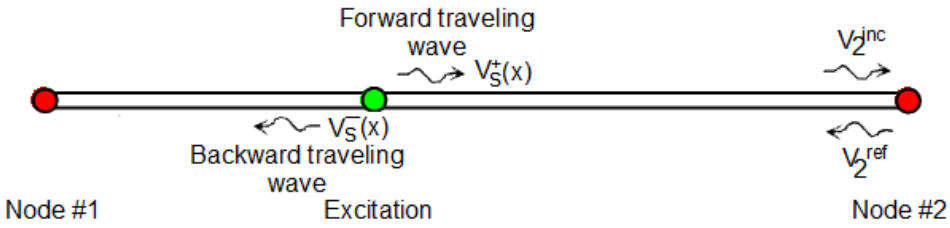

Figure 2.3 Positive and negative traveling waves excited by the sources at $x=x_s$

Without excitation sources, the positive traveling voltage wave at junction#2 is written in terms of the positive voltage traveling wave at junction#1 as

$$V_2^+=V_1^+e^{\gamma L} \quad . \qquad \text{(2.6)}$$

With the existence of the excitation sources, an additional component due to the positive traveling wave is added to V_2^+ as below:

$$V_2^+ \;=\; V_1^+e^{-\gamma L} \;+\; \frac{1}{2}(V_s+Z_c I_s)e^{-\gamma(L-x_s)} \qquad \text{(2.7)}$$

Similarly, the negative traveling wave at junction#1 can be expressed as

$$V_1^- \;=\; V_2^-e^{-\gamma L} \;-\; \frac{1}{2}(V_s-Z_c I_s)e^{-\gamma x_s} \qquad \text{(2.8)}$$

Using equations (2.6), (2.7) and (2.8), *incident* voltage waves at the junctions can be put in a matrix equation form as

$$\begin{bmatrix} V_1^{inc} \\ V_2^{inc} \end{bmatrix}=\begin{bmatrix} 0 & e^{-\gamma L} \\ e^{-\gamma L} & 0 \end{bmatrix}\begin{bmatrix} V_1^{ref} \\ V_2^{ref} \end{bmatrix}+\begin{bmatrix} \frac{-1}{2}(V_s-Z_c I_s)e^{-\gamma x_s} \\ \frac{1}{2}(V_s+Z_c I_s)e^{-\gamma(L-x_s)} \end{bmatrix} \quad .(2.9)$$

According to the transmission line theory, relation between the reflected and incident voltage waves is

$$V^{ref}=\rho V^{inc} \quad , \qquad \text{(2.11)}$$

where ρ is the voltage reflection coefficient and it is defined as

$$\rho = \frac{Z_L - Z_c}{Z_L + Z_c} \quad . \tag{2.12}$$

In Eq. (2.12) Z_L is the load impedance and Z_c is the characteristic impedance of the transmission line connected to the load. For our transmission line network, the vector of reflected voltages can be written by multiplying the reflection coefficient matrix and the vector of incident voltages as

$$\begin{bmatrix} V_1^{ref} \\ V_2^{ref} \end{bmatrix} = \begin{bmatrix} \rho_1 & 0 \\ 0 & \rho_2 \end{bmatrix} \begin{bmatrix} V_1^{inc} \\ V_2^{inc} \end{bmatrix} \quad , \tag{2.13}$$

where ρ_1 and ρ_2 are the reflection coefficients at each junction.

Rearranging the terms of Eq. (2.13) gives a similar expression for the vector of incident voltages:

$$\begin{bmatrix} V_1^{inc} \\ V_2^{inc} \end{bmatrix} = \begin{bmatrix} \rho_1 & 0 \\ 0 & \rho_2 \end{bmatrix}^{-1} \begin{bmatrix} V_1^{ref} \\ V_2^{ref} \end{bmatrix} \quad . \tag{2.14}$$

Substitute Eq.(2.14) into Eq.(2.9) as

$$\begin{bmatrix} \rho_1 & 0 \\ 0 & \rho_2 \end{bmatrix}^{-1} \begin{bmatrix} V_1^{ref} \\ V_2^{ref} \end{bmatrix} = \begin{bmatrix} 0 & e^{-\gamma L} \\ e^{-\gamma L} & 0 \end{bmatrix} \begin{bmatrix} V_1^{ref} \\ V_2^{ref} \end{bmatrix} + \begin{bmatrix} \frac{-1}{2}\left(V_s - Z_c I_s\right) e^{-\gamma x_s} \\ \frac{1}{2}\left(V_s + Z_c I_s\right) e^{-\gamma (L - x_s)} \end{bmatrix} \quad , \tag{2.15}$$

and put the terms with reflected voltage vector on the same side as

$$\begin{bmatrix} \rho_1 & 0 \\ 0 & \rho_2 \end{bmatrix}^{-1} \begin{bmatrix} V_1^{ref} \\ V_2^{ref} \end{bmatrix} - \begin{bmatrix} 0 & e^{-\gamma L} \\ e^{-\gamma L} & 0 \end{bmatrix} \begin{bmatrix} V_1^{ref} \\ V_2^{ref} \end{bmatrix} = \begin{bmatrix} \frac{-1}{2}\left(V_s - Z_c I_s\right) e^{-\gamma x_s} \\ \frac{1}{2}\left(V_s + Z_c I_s\right) e^{-\gamma (L - x_s)} \end{bmatrix} \quad . \tag{2.16}$$

Then multiplying each side by

$$\begin{bmatrix} \rho_1 & 0 \\ 0 & \rho_2 \end{bmatrix}$$

and solving the equation for the reflected voltage vector the BLT equation for the reflected voltages is obtained:

$$\begin{bmatrix} V_1^{ref} \\ V_2^{ref} \end{bmatrix} = \left\{ \begin{bmatrix} 1 & 0 \\ 0 & 1 \end{bmatrix} - \begin{bmatrix} \rho_1 & 0 \\ 0 & \rho_2 \end{bmatrix} \begin{bmatrix} 0 & e^{-\gamma L} \\ e^{-\gamma L} & 0 \end{bmatrix} \right\}^{-1} \times \begin{bmatrix} \rho_1 & 0 \\ 0 & \rho_2 \end{bmatrix} \times \begin{bmatrix} \frac{-1}{2}(V_s - Z_c I_s) e^{-\gamma x_s} \\ \frac{1}{2}(V_s + Z_c I_s) e^{-\gamma (L - x_s)} \end{bmatrix} \tag{2.17}$$

As it can be seen in Eq.(2.17), all reflected voltage waves can be calculated with a single equation by using reflection coefficients, transmission(propagation) coefficients and the source vector.

Once reflected voltages are calculated, incident voltages can be solved from Eq.(2.9) and total voltage vector is obtained as

$$\begin{bmatrix} V_1 \\ V_2 \end{bmatrix} = \begin{bmatrix} V_1^{inc} \\ V_2^{inc} \end{bmatrix} + \begin{bmatrix} V_1^{ref} \\ V_2^{ref} \end{bmatrix} \tag{2.18}$$

Consequently, the BLT equation system can be written as by putting equations (2.9), (2.17) and (2.18) together as an equation system as

$$[V(0)] = ([I] - [S] \times [\Gamma])^{-1} \times [S] \times [V_S] \tag{2.19a}$$

$$[V(L)] = [\Gamma] \times [V(0)] + [V_S] \tag{2.19b}$$

$$[V_{total}] = [V(0)] + [V(L)] \tag{2.19c}$$

where

$[\Gamma]$: the propagation supermatrix,

$[S]$: the scattering supermatrix,

$[V_S]$: the source supervector,

$[V(L)]$: the incident wave matrix, and

$[V(0)]$: the reflected wave matrix.

2.5.2.2 Generalized form of the BLT Equation

The voltage BLT equation system (2.19) is derived from a single transmission line network, and can be used also for more general multiconductor networks. Since EMT models an EM problem as a multiconductor transmission line network consisting of junctions and tubes, the voltage BLT equation system can be generalized for all type of electromagnetic waves and solved by using the scattering parameters at the junctions, propagation parameters at the tubes and EM sources in the system as following

$$[W(0)] = ([I] - [S] \times [\Gamma])^{-1} \times [S] \times [W_S] \tag{2.20a}$$

$$[W(L)]=[\Gamma]\times[W(0)]+[W_S] \tag{2.20b}$$

$$[W_{total}]=[W(0)]+[W(L)] \tag{2.20c}$$

where,

$[\Gamma]$: the propagation supermatrix of the tubes,

$[S]$: the scattering supermatrix of the junctions,

$[W_S]$: the source supervector,

$[W(L)]$: the incident wave matrix, and

$[W(0)]$: the reflected wave matrix.

CHAPTER 3

APPLICATION OF THE EMT METHOD BASED ON BLT EQUATION TO A BRANCH-LINE COUPLER AS A KNOWN SYSTEM

3.1 Branch-Line Coupler

A branch-line coupler is a 3dB directional coupler with 90° phase difference in its through and cross outputs. The geometry of the branch-line coupler is shown in Figure 3.1. When all ports are matched, input power on port 1 is evenly divided between ports 2 and 3 with 90° phase difference. There is no power coupled to isolated port 4.

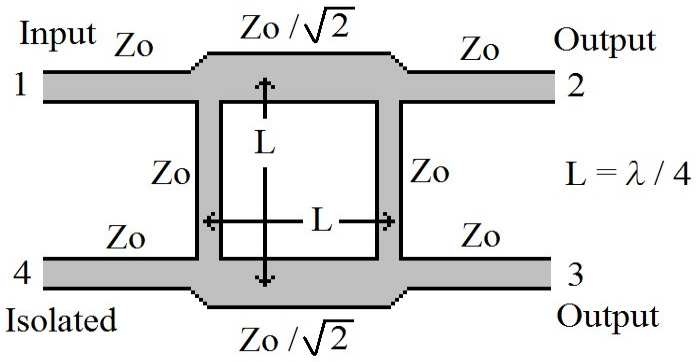

Figure 3.1 Geometry of a branch-line coupler

We can write the voltages on the ports as follows:

Port 1: $V_{in}\angle 0^{\circ}$ (Input)

Port 2: $\frac{1}{\sqrt{(2)}}\ V_{in}\angle -90^{\circ}$ (Output)

Port 3: $\frac{1}{\sqrt{(2)}}\ V_{in}\angle -180^{\circ}$ (Output)

Port 4: 0 (Isolated)

Therefore, the [S] matrix will be as below:

$$[S] = \frac{-1}{\sqrt{(2)}} \begin{bmatrix} 0 & j & 1 & 0 \\ j & 0 & 0 & 1 \\ 1 & 0 & 0 & j \\ 1 & 0 & 0 & j \end{bmatrix} \qquad (3.1)$$

As it can be seen in the Figure 1, branch-line coupler has a high degree symmetry. So, any port can be used as the input port. Then the output ports will be always the through and cross outputs with respect to the input port, and the isolated port will be the remaining port which is on the same side with the input port.

3.2 Even-Odd Mode Analysis

In Figure 2, the schematic circuit of the branch-line coupler is shown in the normalized form. Each circle represents a junction of transmission lines and characteristic impedance of each transmission line normalized to Z_o.

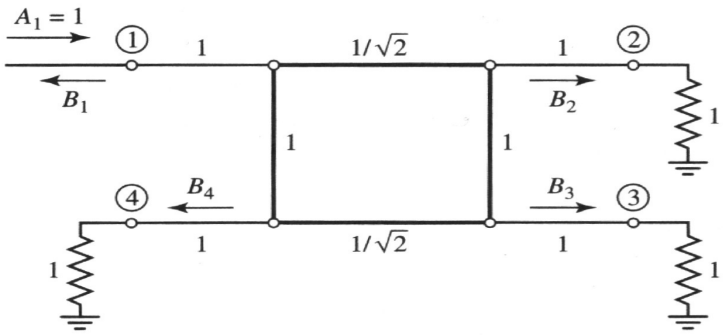

Figure 3.2 Circuit of the branch-line coupler in normalized form

The circuit in Figure 3.2 can be decomposed into the even and odd mode excitations as shown in Figure 3.3. Since the circuit of branch-line coupler is linear, superposition of the even and odd mode excitations gives the original excitation of branch-line coupler. The actual output waves can be obtained by summing the waves at the outputs of the both two excitations.

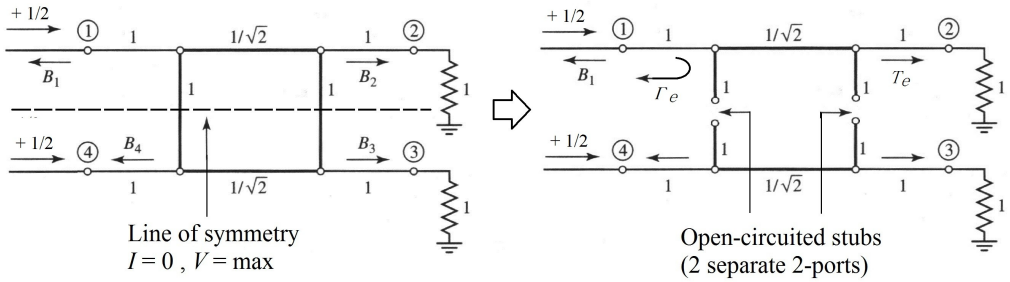

(a)

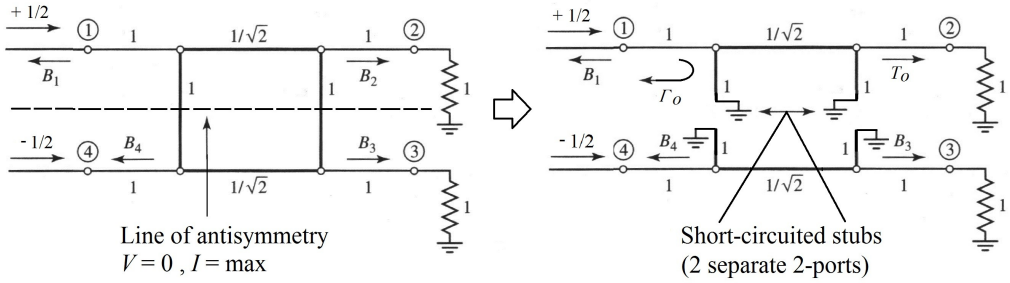

Figure 3.3 Decomposition of the Branch-Line Coupler into Even- and Odd- Mode Excitations (a) Even-mode (e) (b) Odd-mode (o)

As it is shown in Figure 3, the four-port network is decomposed into a set of two decoupled two-port networks. Amplitudes of the incident waves for these two-port networks are $\pm 1/2$, therefore the amplitudes of the resultant waves at each port of the branch-line coupler can be written as

$$B_1 = \frac{1}{2}\Gamma_e + \frac{1}{2}\Gamma_o \qquad (3.2a)$$

$$B_2 = \frac{1}{2}T_e + \frac{1}{2}T_o \qquad (3.2b)$$

$$B_3 = \frac{1}{2}T_e - \frac{1}{2}T_o \qquad (3.2c)$$

$$B_4 = \frac{1}{2}\Gamma_e - \frac{1}{2}\Gamma_o \qquad (3.2d)$$

where Γ_e , Γ_o are reflection coefficients and T_e , T_o transmission coefficients of the two port even and odd mode excitations.

First, calculate the Γ_e and T_e for the two port even-mode circuit by using the ABCD matrices. Even-mode circuit is composed by one λ/4 transmission line and two shunt open-circuited λ/8 stubs on the two ends of this line. Thus, ABCD matrix of the circuit can be found by multiplying ABCD matrices of these three parts as follows:

$$\begin{bmatrix} A & B \\ C & D \end{bmatrix}_e = \begin{bmatrix} 1 & 0 \\ j & 1 \end{bmatrix} \begin{bmatrix} 0 & j/\sqrt{2} \\ j\sqrt{2} & 0 \end{bmatrix} \begin{bmatrix} 1 & 0 \\ j & 1 \end{bmatrix} = \frac{1}{\sqrt{2}} \begin{bmatrix} -1 & j \\ j & -1 \end{bmatrix} \qquad (3.3)$$

where,

$\begin{bmatrix} 1 & 0 \\ j & 1 \end{bmatrix}$: *ABCD* matrix of the one shunt open-circuited λ/8 stub,

$\begin{bmatrix} 0 & j/\sqrt{2} \\ j\sqrt{2} & 0 \end{bmatrix}$: *ABCD* matrix of the λ/4 transmission line.

Then, we can convert ABCD parameters to S parameters, which are equivalent to the reflection and transmission coefficients. So,

$$\Gamma_e = \frac{A+B-C-D}{A+B+C+D} = \frac{(-1+j-j+1)/\sqrt{2}}{(-1+j+j-1)/\sqrt{2}} = 0 \qquad (3.4a)$$

$$T_e = \frac{2}{A+B+C+D} = \frac{2}{(-1+j+j-1)/\sqrt{2}} = -\frac{1}{\sqrt{2}}(1+j) \qquad (3.4b)$$

Similarly, we can write the odd mode *ABCD* parameters as

$$\begin{bmatrix} A & B \\ C & D \end{bmatrix}_o = \frac{1}{\sqrt{2}} \begin{bmatrix} 1 & j \\ j & 1 \end{bmatrix} \qquad (3.5)$$

and the reflection and transmission coefficients as

$$\Gamma_o = 0 \qquad (3.6a)$$

$$T_o = \frac{1}{\sqrt{2}}(1-j) \qquad (3.6b)$$

Then, by putting (3.3) and (3.5) into (3.1) we can get the following output wave results:

$B_1 = 0$ (port 1 is matched), (3.7a)

$B_2 = -\frac{j}{\sqrt{2}}$ (half-power, -90° phase shift from port 1 to 2), (3.7b)

$B_3 = -\frac{1}{\sqrt{2}}$ (half-power, -180° phase shift from port 1 to 3), (3.7c)

$B_4 = 0$ (no-power, isolated port). (3.7d)

3.3 Analysis by EMT based on BLT equation

3.3.1 Topology Diagram of the Branch-Line Coupler

In order to define the topological diagram of the system, first we need to define junctions and tubes. In our problem, tubes represent the transmission lines in the circuit and junctions represent the conjunction point of the transmission lines. Figure 3.4 shows the topological diagram of the problem. In the figure, the incident and reflected waves at the tubes are also shown. The topological diagram consists of six junctions, eight tubes and source.

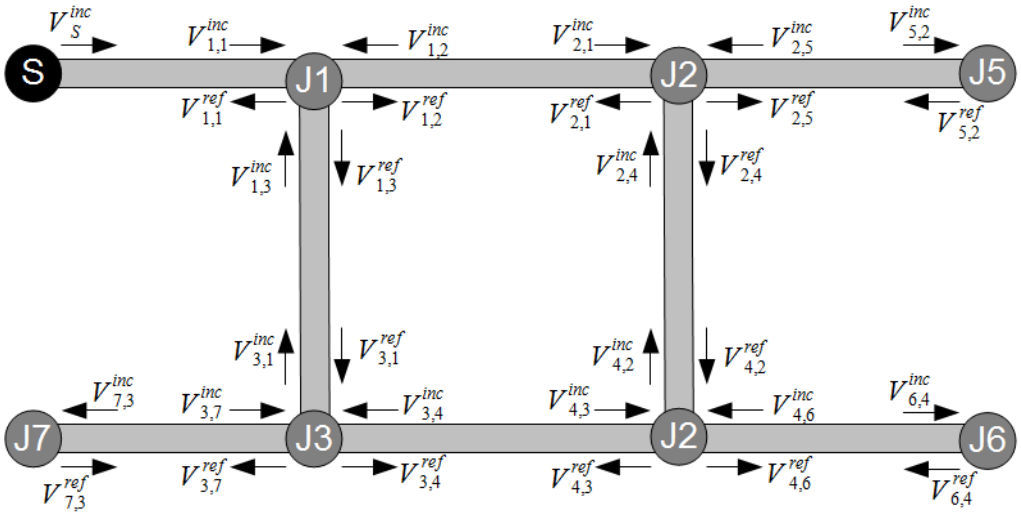

Figure 3.4 The Topological Diagram of the Branch-Line Coupler

After modeling the topological diagram, BLT equation system of the branch-line coupler can be written as below:

$$[V(0)]=([I]-[S]\times[\Gamma])^{-1}\times[S]\times[V_S] \quad (3.8a)$$

$$[V(L)]=[\Gamma]\times[V(0)]+[V_S] \quad (3.8b)$$

$$[V_{total}]=[V(0)]+[V(L)] \quad (3.8c)$$

Where,

$[\Gamma]$: the propagation supermatrix of the tubes,

$[S]$: the scattering supermatrix of the junctions,

$[V_S]$: the source supervector,

$[V(L)]$: the incident wave matrix, and

$[V(0)]$: the reflected wave matrix.

3.3.2 Propagation Supermatrix at the Tubes

Since all tubes in the diagram represent transmission lines, entries of the propagation supermatrix are related to the propagation constants of the tubes.

$$
\begin{bmatrix} V^{inc}_{1,1} \\ V^{inc}_{1,2} \\ V^{inc}_{1,3} \\ V^{inc}_{2,1} \\ V^{inc}_{2,4} \\ V^{inc}_{2,5} \\ V^{inc}_{3,1} \\ V^{inc}_{3,4} \\ V^{inc}_{3,7} \\ V^{inc}_{4,2} \\ V^{inc}_{4,3} \\ V^{inc}_{4,6} \\ V^{inc}_{5,2} \\ V^{inc}_{6,4} \\ V^{inc}_{7,3} \end{bmatrix}
=
\begin{bmatrix}
\Gamma(J1) & & & 0 & 0 & 0 & 0 & 0 & 0 & 0 & 0 & 0 & 0 & 0 \\
 & & & 0 & 0 & 0 & 0 & 0 & 0 & 0 & 0 & 0 & 0 & 0 \\
 & & & 0 & 0 & 0 & 0 & 0 & 0 & 0 & 0 & 0 & 0 & 0 \\
0 & 0 & 0 & \Gamma(J2) & & & 0 & 0 & 0 & 0 & 0 & 0 & 0 & 0 \\
0 & 0 & 0 & & & & 0 & 0 & 0 & 0 & 0 & 0 & 0 & 0 \\
0 & 0 & 0 & & & & 0 & 0 & 0 & 0 & 0 & 0 & 0 & 0 \\
0 & 0 & 0 & 0 & 0 & 0 & \Gamma(J3) & & & 0 & 0 & 0 & 0 & 0 \\
0 & 0 & 0 & 0 & 0 & 0 & & & & 0 & 0 & 0 & 0 & 0 \\
0 & 0 & 0 & 0 & 0 & 0 & & & & 0 & 0 & 0 & 0 & 0 \\
0 & 0 & 0 & 0 & 0 & 0 & 0 & 0 & 0 & \Gamma(J4) & & & 0 & 0 & 0 \\
0 & 0 & 0 & 0 & 0 & 0 & 0 & 0 & 0 & & & & 0 & 0 & 0 \\
0 & 0 & 0 & 0 & 0 & 0 & 0 & 0 & 0 & & & & 0 & 0 & 0 \\
0 & 0 & 0 & 0 & 0 & 0 & 0 & 0 & 0 & 0 & 0 & 0 & \Gamma(J4) & & \\
0 & 0 & 0 & 0 & 0 & 0 & 0 & 0 & 0 & 0 & 0 & 0 & & & \\
0 & 0 & 0 & 0 & 0 & 0 & 0 & 0 & 0 & 0 & 0 & 0 & & &
\end{bmatrix}
\begin{bmatrix} V^{ref}_{1,1} \\ V^{ref}_{1,2} \\ V^{ref}_{1,3} \\ V^{ref}_{2,1} \\ V^{ref}_{2,4} \\ V^{ref}_{2,5} \\ V^{ref}_{3,1} \\ V^{ref}_{3,4} \\ V^{ref}_{3,7} \\ V^{ref}_{4,2} \\ V^{ref}_{4,3} \\ V^{ref}_{4,6} \\ V^{ref}_{5,2} \\ V^{ref}_{6,4} \\ V^{ref}_{7,3} \end{bmatrix}
\tag{3.9}
$$

3.3.3 Scattering Supermatrix at the Junctions

The scattering supermatrix of the system consists of scattering matrices of the junctions. After we calculate the scattering matrices of each junction separately, we can reconstruct the whole system by constructing the supermatrix as in Eq. (3.10).

$$
\begin{bmatrix} V^{ref}_{1,1} \\ V^{ref}_{1,2} \\ V^{ref}_{1,3} \\ V^{ref}_{2,1} \\ V^{ref}_{2,4} \\ V^{ref}_{2,5} \\ V^{ref}_{3,1} \\ V^{ref}_{3,4} \\ V^{ref}_{3,7} \\ V^{ref}_{4,2} \\ V^{ref}_{4,3} \\ V^{ref}_{4,6} \\ V^{ref}_{5,2} \\ V^{ref}_{6,4} \\ V^{ref}_{7,3} \end{bmatrix}
=
\begin{bmatrix}
S(J1) & & & 0 & 0 & 0 & 0 & 0 & 0 & 0 & 0 & 0 & 0 & 0 \\
 & & & 0 & 0 & 0 & 0 & 0 & 0 & 0 & 0 & 0 & 0 & 0 \\
 & & & 0 & 0 & 0 & 0 & 0 & 0 & 0 & 0 & 0 & 0 & 0 \\
0 & 0 & 0 & S(J2) & & & 0 & 0 & 0 & 0 & 0 & 0 & 0 & 0 \\
0 & 0 & 0 & & & & 0 & 0 & 0 & 0 & 0 & 0 & 0 & 0 \\
0 & 0 & 0 & & & & 0 & 0 & 0 & 0 & 0 & 0 & 0 & 0 \\
0 & 0 & 0 & 0 & 0 & 0 & S(J3) & & & 0 & 0 & 0 & 0 & 0 \\
0 & 0 & 0 & 0 & 0 & 0 & & & & 0 & 0 & 0 & 0 & 0 \\
0 & 0 & 0 & 0 & 0 & 0 & & & & 0 & 0 & 0 & 0 & 0 \\
0 & 0 & 0 & 0 & 0 & 0 & 0 & 0 & 0 & S(J4) & & & 0 & 0 & 0 \\
0 & 0 & 0 & 0 & 0 & 0 & 0 & 0 & 0 & & & & 0 & 0 & 0 \\
0 & 0 & 0 & 0 & 0 & 0 & 0 & 0 & 0 & & & & 0 & 0 & 0 \\
0 & 0 & 0 & 0 & 0 & 0 & 0 & 0 & 0 & 0 & 0 & 0 & S(J4) & & \\
0 & 0 & 0 & 0 & 0 & 0 & 0 & 0 & 0 & 0 & 0 & 0 & & & \\
0 & 0 & 0 & 0 & 0 & 0 & 0 & 0 & 0 & 0 & 0 & 0 & & &
\end{bmatrix}
\begin{bmatrix} V^{inc}_{1,1} \\ V^{inc}_{1,2} \\ V^{inc}_{1,3} \\ V^{inc}_{2,1} \\ V^{inc}_{2,4} \\ V^{inc}_{2,5} \\ V^{inc}_{3,1} \\ V^{inc}_{3,4} \\ V^{inc}_{3,7} \\ V^{inc}_{4,2} \\ V^{inc}_{4,3} \\ V^{inc}_{4,6} \\ V^{inc}_{5,2} \\ V^{inc}_{6,4} \\ V^{inc}_{7,3} \end{bmatrix}
\tag{3.10}
$$

Scattering parameters of each junction is calculated by the calculation technique for multiconductor transmission line networks which is proposed by Parmantier [27]. Parmantier defined the scattering matrix of a junction as

$$S=\begin{bmatrix} -C_V \\ C_I \cdot Y_c \end{bmatrix}^{-1} \cdot \begin{bmatrix} C_V \\ C_I \cdot Y_c \end{bmatrix} \tag{3.11}$$

where Y_c is the characteristic admittance vector of the junction and C_V is the matrix which satisfies the Kirchoff's voltage equation (3.12) at the junction.

$$C_V \cdot V = 0 \tag{3.12}$$

The size of the matrix is $N_V \times N$ where N_V is the number of nodes for which Kirchoff's voltage equation can be written and N is the total number of ports at the junction. Similarly, C_I is the matrix which satisfies the Kirchoff's current equation (3.13) at the junction.

$$C_I \cdot V = 0 \tag{3.13}$$

The size of the matrix is $N_I \times N$ where N_I is the number of nodes for which Kirchoff's current equation can be written and N is the total number of ports at the junction as above.

In this calculation technique, junctions are classified as short-circuit junction, open-circuit junction, combined short-circuit and open-circuit junction, combined short-circuit and transmission junction, combined open-circuit and transmission junction and fork junction. Each junction of our topological diagram is a fork junction as in Figure 3.5.

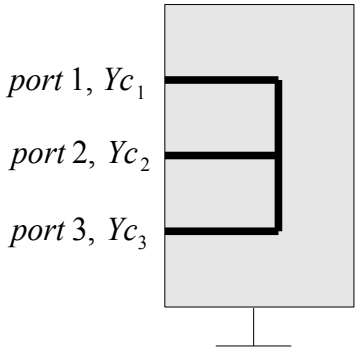

Figure 3.5 Fork Junction

For the a fork junction $N_V = 2$ and $N_c = 1$. So we can write the matrices a C_V and C_I as follows:

$$C_V=\begin{bmatrix}1 & -1 & 0\\ 1 & 0 & -1\end{bmatrix} \quad (3.14a)$$

$$C_I=\begin{bmatrix}1 & 1 & 0\end{bmatrix} \quad (3.14b)$$

Then, by using C_V and C_I S matrix can be calculated as below:

$$S=\begin{bmatrix}-1 & 1 & 0\\ -1 & 0 & 1\\ Yc_1 & Yc_2 & Yc_3\end{bmatrix}^{-1}\cdot\begin{bmatrix}1 & -1 & 0\\ 1 & 0 & -1\\ Yc_1 & Yc_2 & Yc_3\end{bmatrix}=$$

$$\frac{1}{Yc_1+Yc_2+Yc_3}\cdot\begin{bmatrix}Yc_1-Yc_2-Yc_3 & 2\mathrm{Yc}_2 & 2\mathrm{Yc}_3\\ 2\mathrm{Yc}_1 & Yc_2-Yc_1-Yc_3 & 2\mathrm{Yc}_3\\ 2\mathrm{Yc}_1 & 2\mathrm{Yc}_2 & Yc_3-Yc_1-Yc_2\end{bmatrix} \quad (3.15)$$

Applying the equation (3.15) to the junction of the topological diagram of branch-line coupler in Figure 4, we find the scattering matrices of the junctions as below:

$$S(J1)=\frac{1}{(1+\sqrt{2}+1)Y_0}\cdot\begin{bmatrix}(1-\sqrt{2}-1)Y_0 & 2\sqrt{2}Y_0 & 2\mathrm{Y}_0\\ 2\mathrm{Y}_0 & (\sqrt{2}-1-1)Y_0 & 2\mathrm{Y}_0\\ 2\mathrm{Y}_0 & 2\sqrt{2}Y_0 & (1-\sqrt{2}-1)Y_0\end{bmatrix}$$

$$=\frac{1}{2+\sqrt{2}}\cdot\begin{bmatrix}-\sqrt{2} & 2\sqrt{2} & 2\\ 2 & \sqrt{2}-2 & 2\\ 2 & 2\sqrt{2} & -\sqrt{2}\end{bmatrix}$$

$$S(J1)=\frac{1}{\sqrt{2}+1}\cdot\begin{bmatrix}-1 & 2 & \sqrt{2}\\ \sqrt{2} & 1-\sqrt{2} & \sqrt{2}\\ \sqrt{2} & 2 & -1\end{bmatrix}$$

Similarly,

$$S(J2)=\frac{1}{\sqrt{2}+1}\cdot\begin{bmatrix}1-\sqrt{2} & \sqrt{2} & \sqrt{2}\\ 2 & -1 & \sqrt{2}\\ 2 & \sqrt{2} & -1\end{bmatrix}$$

$$S(J3)=S(J1)=\frac{1}{\sqrt{2}+1}\cdot\begin{bmatrix}-1 & 2 & \sqrt{2}\\ \sqrt{2} & 1-\sqrt{2} & \sqrt{2}\\ \sqrt{2} & 2 & -1\end{bmatrix}$$

$$S(J4)=\frac{1}{\sqrt{2}+1}\cdot\begin{bmatrix}-1 & \sqrt{2} & 2\\ \sqrt{2} & -1 & 2\\ \sqrt{2} & \sqrt{2} & 1-\sqrt{2}\end{bmatrix}$$

3.3.4 Results

While solving the branch-line coupler by EMT based on BLT equation, source is taken as unit source for simplicity. Then, outgoing waves at the junctions is found as following:

$$
\begin{bmatrix}
V^{ref}_{1,1} \\ V^{ref}_{1,2} \\ V^{ref}_{1,3} \\ V^{ref}_{2,1} \\ V^{ref}_{2,4} \\ V^{ref}_{2,5} \\ V^{ref}_{3,1} \\ V^{ref}_{3,4} \\ V^{ref}_{3,7} \\ V^{ref}_{4,2} \\ V^{ref}_{4,3} \\ V^{ref}_{4,6} \\ V^{ref}_{5,2} \\ V^{ref}_{6,4} \\ V^{ref}_{7,3}
\end{bmatrix}
=
\begin{bmatrix}
-0.5468+0.00000\mathrm{i} \\
0.4375+4.1199\text{e-}18\,i \\
0.75+8.2399\text{e-}18\,i \\
-3.4694\text{e-}18+0.0000\mathrm{i} \\
2.0816\text{e-}17-0.125\mathrm{i} \\
-0.7071\mathrm{i} \\
-6.9388\text{e-}18+0.125\mathrm{i} \\
2.0816\text{e-}17-0.1875\mathrm{i} \\
0 \\
-0.125 \\
-0.125-2.7755\text{e-}17\,i \\
-0.7071 \\
0 \\
0 \\
0
\end{bmatrix}
$$

As it is seen in the equation, BLT solves all outgoing waves however for branch-line coupler we need only $V^{ref}_{2,5}$, $V^{ref}_{4,6}$ and, $V^{ref}_{3,7}$ since they are the output voltages of port-2, port-3 and port-4 respectively. Magnitudes and angles of these three port voltages are as below:

$V^{ref}_{2,5}$ = 0.701 ∟-90° (Port-2)

$V^{ref}_{4,6}$ = 0.701 ∟-180° (Port-)

$V^{ref}_{3,7}$ = 0 (Isolated)

Consequently, it can be seen that EMT results are same with the even- and odd- mode analysis results. We see that BLT can solve such a multiconductor network by using only junction scattering parameters and tube propagation parameters properly. For more complex systems EMT can simplify the analysis of the system. Sometimes scattering parameters of some sub-systems or components are already given in the datasheets or can be easily found by simulation tools. In addition, propagation parameters are generally characterized by the transmission-line, free-space or waveguide parameters. Thus, for a complex system voltage, current or electromagnetic waves at any point of the system can be calculated easily and fast by EMT based on BLT equation.

CHAPTER 4

ANALYSIS of SHIELDING BOXES by EMT BASED on BLT EQUATION AND SIMULATION WITH CST MICROWAVE STUDIO®

In this chapter, analysis of shielding boxes with electromagnetic topology based on BLT equation will be introduced and results will be compared with the simulation results obtained with CST MICROWAVE STUDIO®. We will analyze rectangular shielding boxes with rectangular aperture illuminated by a plane wave at normal incidence as shown in Figure 4.1. They are all made by perfect electric conductor with zero thickness and have only one rectangular aperture at the center of their front faces. Electric field polarization of the incident plane wave is in y-direction. In order to verify the method boxes with different sizes and with different aperture dimensions are analyzed.

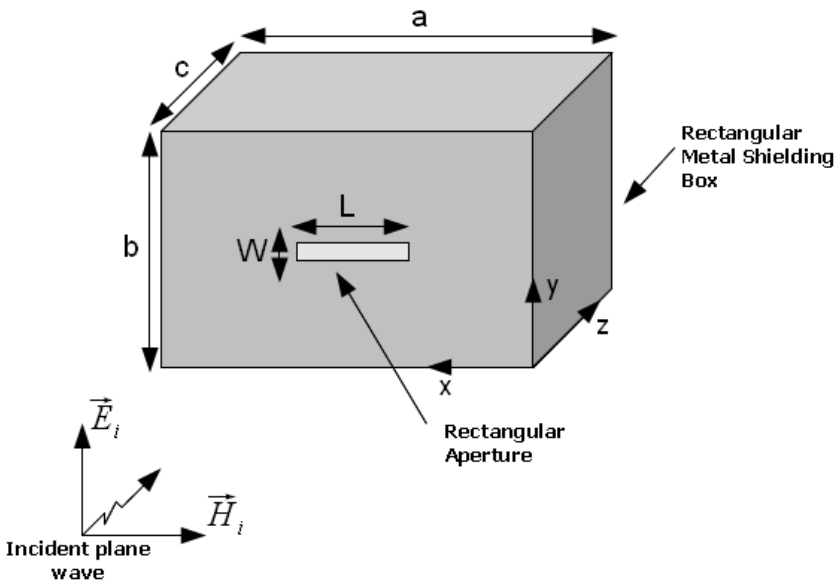

Figure 4.1 Geometry of rectangular shielding box with rectangular aperture illuminated by a plane wave at normal incidence

At the end of the chapter, simulations of the boxes are also performed in CST MICROWAVE STUDIO® and outputs are compared with the analysis results.

4.1. Analysis by EMT based on BLT equation

As mentioned in previous chapters, BLT equation is basically used for multiconductor network systems. However, it can be used for all systems that can be modeled as a

multiconductor network system. This can be done by using electromagnetic topology which divides the system into smaller parts as junctions and tubes connecting these junctions. After modeling the system as a network consisting of junction and tubes, it can be reconstructed and all outgoing and incoming waves at the junctions can be solved by BLT equation system (4.1). Then, one can calculate the total waves by summing the incoming and outgoing waves.

For shielding box analysis, we can write the BLT equation system of (2.20) as below:

$$[E^{ref}]=([I]-[S]\times[\Gamma])^{-1}\times[S]\times[E_S] \quad (4.1a)$$

$$[E^{inc}]=[\Gamma]\times[E^{ref}]+[E_S] \quad (4.1b)$$

$$[E_{total}]=[E^{inc}]+[E^{ref}] \quad (4.1c)$$

Where,

$[I]$: unit matrix,

$[\Gamma]$: the propagation supermatrix,

$[S]$: the scattering supermatrix,

$[E_S]$: the source supervector,

$[E^{inc}]$: the incident wave matrix, and

$[E^{ref}]$: the reflected wave matrix.

Once incident and reflected fields found, electric field at any point inside and outside the shielding box can be calculated. We are only interested in the fields inside the box in this thesis. After solving the electric field at a given point inside, using the following SE formula

$$SE=-20\log\left(\frac{|\vec{E}_{\text{int}}|}{|\vec{E}_{\text{ext}}|}\right) \quad (4.2)$$

shielding effectiveness can be calculated, where $\vec{E}_{\text{int}}$ is the electric field at the point inside the shielding box and $\vec{E}_{\text{ext}}$ is the electric field at the same point in absence of the box.

In order to analyze a system by EMT based on BLT equation, topological diagram of the system needs to be defined first. After the definition, scattering and propagating supermatrices of the topology are constructed from the scattering and propagating characteristics of the junctions and tubes respectively.

4.1.1. Modeling of the Topological Diagram

Modeling the topological diagram of a system is the first step of the electromagnetic topology method, which refers to division of the structure of the main system into a set of sub-volumes [1]. In our model, a rectangular shielding box is divided into three parts as front face, back face and side faces. The front face of the box is an infinite PEC plane

with a rectangular aperture, the back face is an infinite PEC plane and side faces constitute a rectangular waveguide as in Figure 4.2.

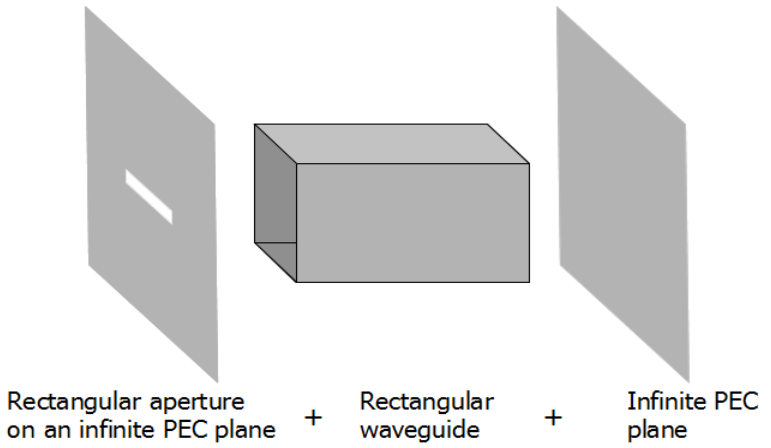

Figure 4.2 Modelling of the shielding box for topological diagram

According to this model, topological diagram is formed as in Figure 4.3. In the topological diagram, shielding box modeled as two junctions and one tube connecting these junctions. One of the junctions is *J2* which characterizes the infinite PEC plane with a rectangular aperture on it and the other one, *J3*, characterizes the infinite PEC plane. Then the characteristics of the tube *T3* are same with the characteristics of the rectangular waveguide. In addition, *J1* characterizes the infinity point and *S* characterizes the source point which radiates plane wave towards the front face of the shielding box. Other tubes *T1* and *T2* have the characteristics of free-space.

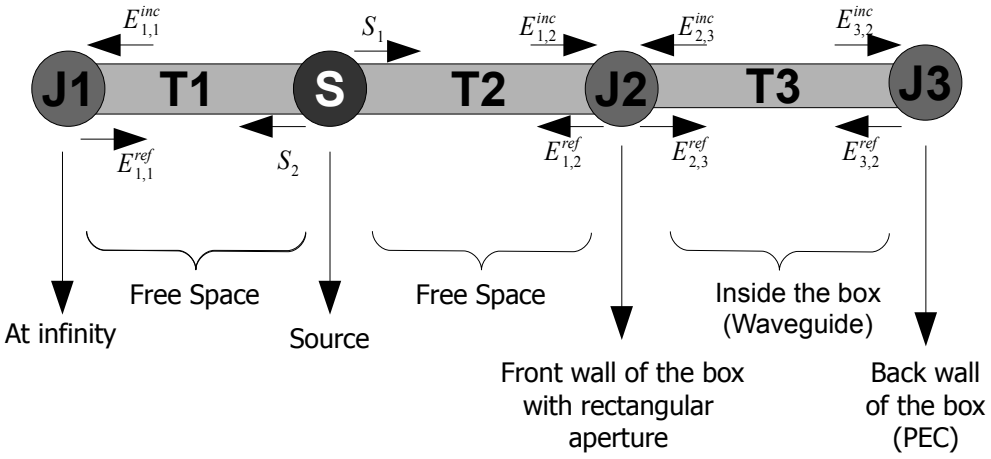

Figure 4.3 The Topological Diagram of the Shielding Box

4.1.2. Propagation Supermatrix at the Tubes

The incident and scattered waves at the tubes are represented as in Figure 4.3 and according to this representation Eq. (4.1b) is formed as

$$\begin{bmatrix} E_{1,1}^{inc} \\ E_{1,2}^{inc} \\ E_{2,3}^{inc} \\ E_{3,2}^{inc} \end{bmatrix} = \begin{bmatrix} \Gamma(T1) & 0 & 0 & 0 \\ 0 & \Gamma(T2) & 0 & 0 \\ 0 & 0 & 0 & \Gamma(T3) \\ 0 & 0 & \Gamma(T3) & 0 \end{bmatrix} \begin{bmatrix} E_{1,1}^{ref} \\ E_{1,2}^{ref} \\ E_{2,3}^{ref} \\ E_{3,2}^{ref} \end{bmatrix} + \begin{bmatrix} S_2 \\ S_1 \\ 0 \\ 0 \end{bmatrix} . \quad (4.3)$$

In the propagation supermatrix in Eq. (4.3) , both $\Gamma(T1)$ and d $\Gamma(T2)$ describes the propagation characteristics of free-space, so they can be written as:

$$\Gamma(T1) = e^{\pm j k_0 z}$$

$$\Gamma(T2) = e^{\pm j k_0 z} \quad .$$

where $k_0 = \omega\sqrt{\mu_0 \varepsilon_0}$.

In addition, since T3 represents a rectangular waveguide according to our model, $\Gamma(T3)$ can be written as

$$\Gamma(T3) = \frac{-j\omega\mu m\pi}{k_c^2 b} A_{mn} \sin\left(\frac{m\pi x}{a}\right) \cos\left(\frac{n\pi y}{b}\right) e^{-j\beta_z z} \qquad (4.4)$$

which is the characteristics of the electric field component of the TE_{mn} mode polarized in y-direction and propagating in z-direction in a rectangular waveguide [28] .

4.1.3. Scattering Supermatrix at the Junctions

The scattering supermatrix is created by using the incident and the reflected waves at each junction in Figure 4.3. Then Eq. (4.1a) takes the following form:

$$\begin{bmatrix} E_{1,1}^{ref} \\ E_{1,2}^{ref} \\ E_{2,3}^{ref} \\ E_{3,2}^{ref} \end{bmatrix} = \begin{bmatrix} S(J1) & 0 & 0 & 0 \\ 0 & S(J2) & S(J2) & 0 \\ 0 & S(J2) & S(J2) & 0 \\ 0 & 0 & 0 & S(J3) \end{bmatrix} \begin{bmatrix} E_{1,1}^{inc} \\ E_{1,2}^{inc} \\ E_{2,3}^{inc} \\ E_{3,2}^{inc} \end{bmatrix} \qquad (4.4)$$

Scattering parameter of a junction is calculated by division of the outgoing waves at that junction to the incoming waves. S_{11} of a junction can be calculated as in Eq. (4.5).

$$S_{11} = \frac{\vec{E}^{\text{ref}}}{\vec{E}_{\text{inc}}} \qquad (4.5)$$

S(J1) represents the one-port s-parameter of the infinity and $S_{11}(J1) = 0$ since there is no reflection from infinity.

Besides, S(J3) represents the PEC plane and has a one port s-parameter $S_{11}(J3) = -1$.

Lastly, S(J2) represents the scattering parameters of the aperture on a PEC ground plane. Scattered field from the aperture needs to be found in order to calculate the scattering parameters of the junction. It is assumed that an incident plane wave with constant amplitude generates a sinusoidal field distribution on the aperture which has an amplitude equal to the amplitude of the incident wave (See Figure 4.4).

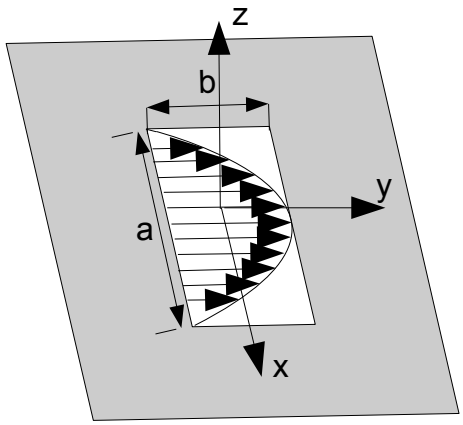

Figure 4.4 Electric field distribution on the aperture

If the incident wave is

$$\vec{E}_{\text{inc}} = \hat{\boldsymbol{a}}_y E_0 e^{-jk_0 z} \quad , \tag{4.6}$$

aperture field can be written as

$$\left.\begin{array}{l} \vec{\boldsymbol{E}}_{\mathbf{a}} = \hat{\boldsymbol{a}}_y E_0 \cos\left(\frac{\pi}{a} x'\right) \\ \end{array}\right\} \begin{array}{l} -a/2 \leqslant x' \leqslant a/2 \\ -b/2 \leqslant y' \leqslant b/2 \end{array} \quad . \tag{4.7}$$

Then an equivalent magnetic current can be written for the aperture:

$$\left.\begin{array}{l} \boldsymbol{M}_s = -2\,\hat{\boldsymbol{n}} \times \vec{\boldsymbol{E}}_{\mathbf{a}} \\ \end{array}\right\} \begin{array}{l} -a/2 \leqslant x' \leqslant a/2 \\ -b/2 \leqslant y' \leqslant b/2 \end{array} \tag{4.8}$$

Due to the equivalent magnetic current in Eq. (4.8), radiated electric field components for far-field can be written as follows [29]:

$$E_r = H_r = 0 \tag{4.9a}$$

$$E_\theta = -\frac{\pi}{2} C \sin\Phi \frac{\cos X}{(X)^2 - \left(\frac{\pi}{2}\right)^2} \frac{\sin Y}{Y} \tag{4.9b}$$

$$E_\Phi = -\frac{\pi}{2} C \cos\theta \cos\Phi \frac{\cos X}{(X)^2 - \left(\frac{\pi}{2}\right)^2} \frac{\sin Y}{Y} \tag{4.9c}$$

where

$$X = \frac{k_0 a}{2} sin\theta cos\Phi$$
$$Y = \frac{k_0 b}{2} sin\theta sin\Phi$$
$$C = j\frac{abk_0 E_0 e^{-jk_0 r}}{2\pi r}$$

Since incident wave is y-polarized and propagating on the z-axis, we need to find the y-polarized reflected wave on the z-axis and then calculate the S-parameters by using Eq. (4.5). If we take the $\theta = 0$ and $\Phi = 90$, electric field will be y-polarized and propagating in -z direction. Then reflected wave from aperture on a PEC ground plane can be written as

$$\vec{E}_y^{ref} = E_\Phi e^{-jk_0 r} = j\frac{abk_0 E_0}{\pi^2 z} e^{-jk_0 z} \quad . \tag{4.10}$$

Then using Eq. (4.5), S_{11} of J2 is calculated as following:

$$S_{11}(J2) = \frac{j\frac{abk_0 E_0}{\pi^2 z}}{E_0} = j\frac{abk_0}{\pi^2 z} \tag{4.11}$$

Since aperture radiates the field to the both sides of the PEC plane, $S_{12}(J2) = -S_{11}(J2)$ and due to the symmetry $S_{22}(J2) = S_{11}(J2)$ and $S_{21}(J2) = S_{12}(J2)$.

4.1.4. BLT equation

After calculation of the propagation and scattering supermatrices, we can write the BLT equation as follows:

$$\begin{bmatrix} E_{1,1}^{ref} \\ E_{1,2}^{ref} \\ E_{2,3}^{ref} \\ E_{3,2}^{ref} \end{bmatrix} = \left([I] - \begin{bmatrix} S_{11}(J1) & 0 & 0 & 0 \\ 0 & S_{11}(J2) & S_{12}(J2) & 0 \\ 0 & S_{21}(J2) & S_{22}(J2) & 0 \\ 0 & 0 & 0 & S_{11}(J3) \end{bmatrix} \times \begin{bmatrix} \Gamma(T1) & 0 & 0 & 0 \\ 0 & \Gamma(T2) & 0 & 0 \\ 0 & 0 & 0 & \Gamma(T3) \\ 0 & 0 & \Gamma(T3) & 0 \end{bmatrix} \right)^{-1}$$
$$\times \begin{bmatrix} S_{11}(J1) & 0 & 0 & 0 \\ 0 & S_{11}(J2) & S_{12}(J2) & 0 \\ 0 & S_{21}(J2) & S_{22}(J2) & 0 \\ 0 & 0 & 0 & S_{11}(J3) \end{bmatrix} \times \begin{bmatrix} S_2 \\ S_1 \\ 0 \\ 0 \end{bmatrix} \tag{4.12}$$

BLT equation in Eq. (4.12) gives all outgoing waves at the junctions. Electric field at the center of the shielding box can be calculated by adding up the wave radiated by aperture into the box $\left(E_{2,3}^{ref}\right)$ and the wave reflected from the back wall of the box $\left(E_{3,2}^{ref}\right)$ at the center of the box.

When electric field at the center of the shielding box is calculated with respect to the frequency, shielding effectiveness of the box can also be calculated.

4.2. EMT Results and Simulation by CST MICROWAVE STUDIO®

In this section, EMT results of electric field component at the center of various shielding boxes are introduced and compared with the simulation results obtained by CST MICROWAVE STUDIO® . All results are shown above the cutoff frequencies of the boxes.

- **Shielding Box-1:**
  Dimensions: 30cm x 12cm x 30cm
  Aperture area: 10 x 0.5 cm^2
  Analysis Frequency Range: 0.5-2.0 GHz

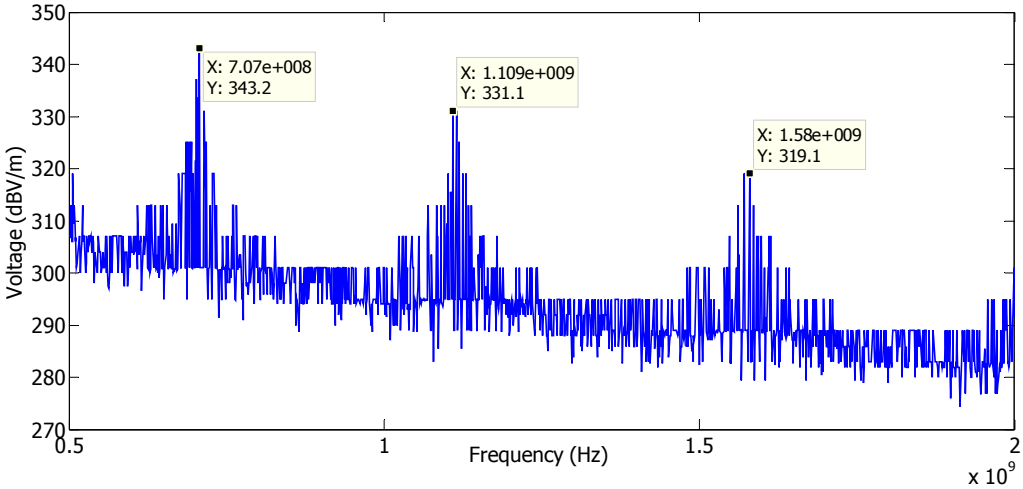

Figure 4.5 EMT analysis result of E-field at the center of 30cmx12cmx30cm shielding box with 10x0.5 cm2 aperture located at the center of its front face.

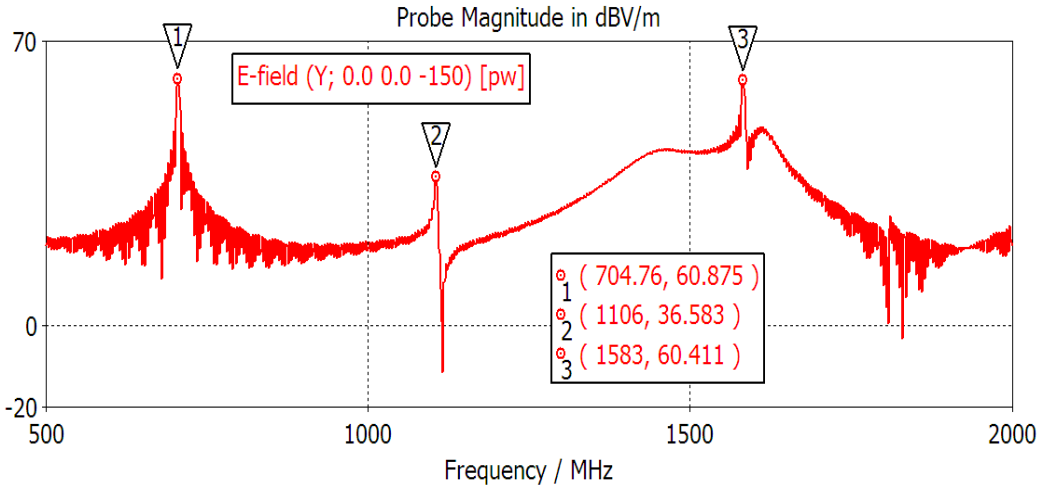

Figure 4.6 CST MICROWAVE STUDIO® simulation result of E-field at the center of 30cmx12cmx30cm shielding box with 10x0.5 cm2 aperture located at the center of its front face.

- **Shielding Box-2:**

  Dimensions: 30cm x 12cm x 30cm
  Aperture area: 10 x 3 cm^2
  Analysis Frequency Range: 0.5-2.0 GHz

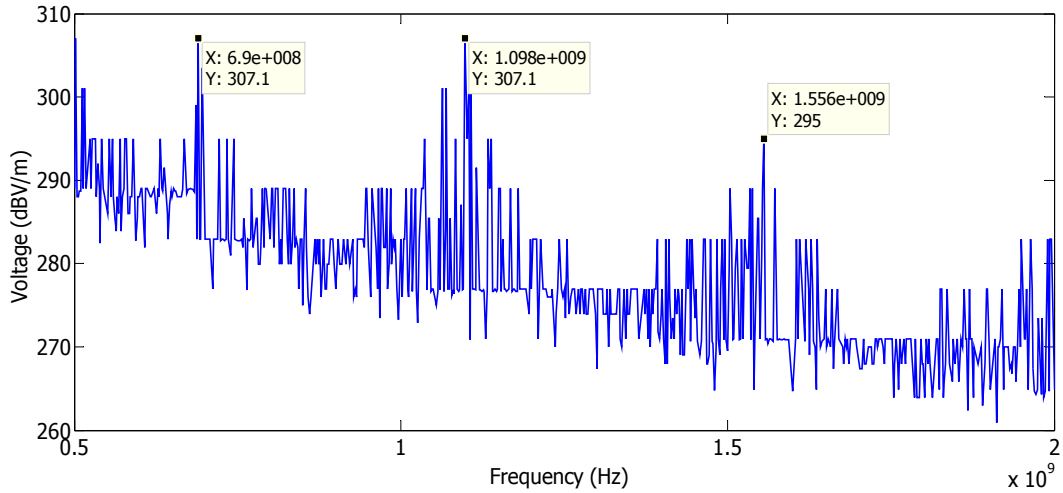

Figure 4.7 EMT analysis result of E-field at the center of 30cmx12cmx30cm shielding box with 10x3 cm2 aperture located at the center of its front face.

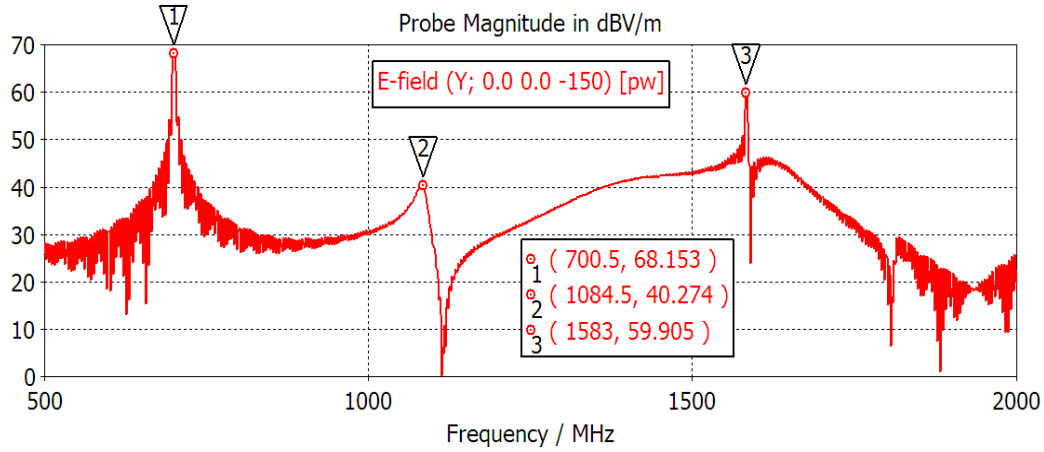

Figure 4.8 CST MICROWAVE STUDIO® simulation result of E-field at the center of 30cmx12cmx30cm shielding box with 10x3 cm2 aperture located at the center of its front face.

- **HP Branded PC Case:**

  Dimensions: 17cm x 45cm x 45cm
  Aperture area: 10 x 2 cm^2
  Analysis Frequency Range: 0.9-2.0 GHz

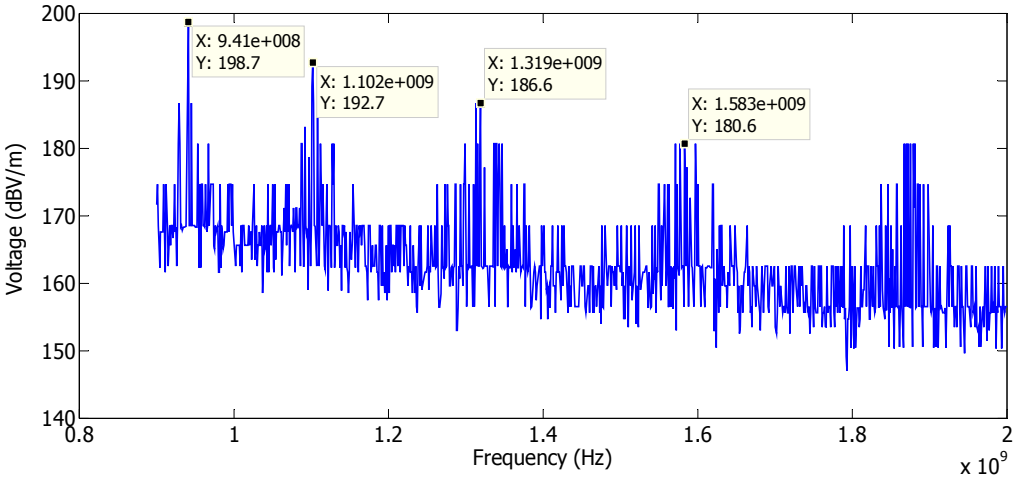

Figure 4.9 EMT analysis result of E-field at the center of 17cmx45cmx45cm PC case with 10x2 cm2 CD driver aperture located at the center of its front face.

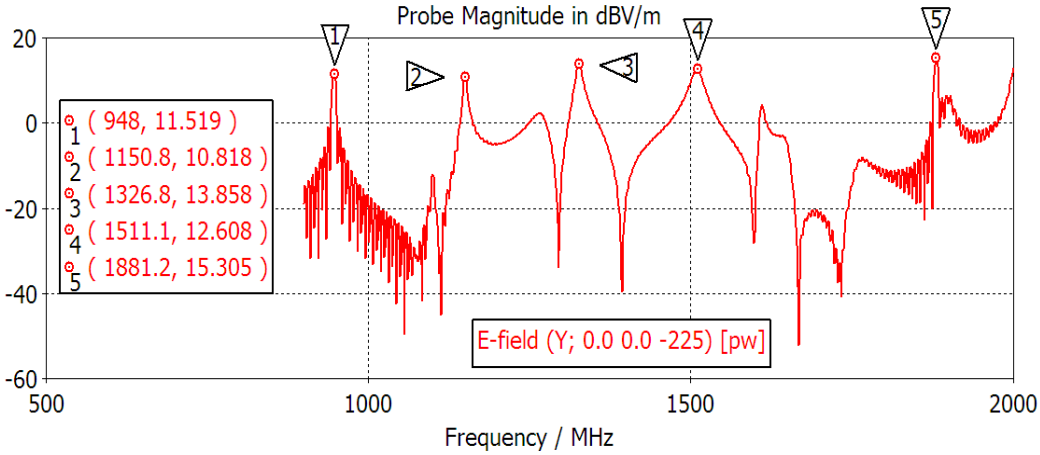

Figure 4.10 CST MICROWAVE STUDIO® simulation result of E-field at the center of 17cmx45cmx45cm PC case with 10x2 cm2 CD driver aperture located at the center of its front face.

Results of EMT method and CST MICROWAVE STUDIO® simulations are tabulated in Table 4.1 in order to see the comparison better.

Shieldin Box	Peak Number	Peak Positions (GHz)		Analysis Duration (sec)	
		EMT Results	CST Results	EMT Method	CST Simulation
Shielding Box-1	1	0.707	0.705	5	600
	2	1.109	1.106		
	3	1.580	1.583		
Shielding Box-2	1	0.690	0.700	5	590
	2	1.098	1.084		
	3	1.556	1.583		
PC Case	1	0.941	0.948	5	370
	2	1.102	1.150		
	3	1.319	1.326		
	4	1.583	1.511		
	5	1.875	1.881		

Table 1 Peak positions of the EMT and CST MICROWAVE STUDIO® simulation results due to the frequency

As it can be seen it the Table 4.1 peak positions of both EMT method and CST MICROWAVE STUDIO® simulations are very close to each other. It is also seen from the same table that EMT solves the problem much faster than the CST MICROWAVE STUDIO® .

CHAPTER 5

CONCLUSION

Shielding is of vital importance in electronics in terms of protection of devices from malfunction or damage caused by EMI issues and also the topic of Tempest applications in terms of information security. Usage of shielding boxes is one of the methods to provide shielding. Assessment of shielding effectiveness of shielding boxes according to size, shape and location of the apertures that may exist on them is an important requirement to design effective shielding boxes. There are several numerical and analytical methods in the literature to calculate SE but they have some drawbacks in terms of accuracy, time or memory.

The main purpose of this thesis was to get an accurate insight of shielding effectiveness of a shielding box at different frequencies in the shortest time and with a minimum memory requirement. This has been accomplished by using EMT method based on BLT equation. Throughout the thesis, EMT method based on BLT equation and its application on assessment of shielding effectiveness of shielding boxes is investigated.

As a first step, EMT method is used for analysis of the branch-line coupler and its application for multiconductor transmission line networks is examined, which is the first application area of the BLT equation. It is seen that BLT is an alternative method for such a multiconductor network and can solve such networks easily, if scattering and propagation parameters of the topological elements (junctions and tubes) are known. It can be used for all multiconductor transmission line networks and all systems that can be modelled as a multiconductor transmission line network consisting of junctions and tubes.

Secondly, usage of EMT method based on BLT equation for assessment of shielding effectiveness of shielding boxes is examined. In order to perform the method, topological network of the system modeled as a first step. EM source radiating incident plane wave towards shielding box and shielding box itself are taken as a system and all EM field interactions in the system modeled by junctions and tubes. Then, scattering and propagation parameters of the junctions and tubes are characterized by a new modeling approach. In our model, a rectangular shielding box is divided into three parts as front face, back face and side faces. The front face of the box is an infinite PEC plane with a rectangular aperture, the back face is an infinite PEC plane and side faces constitute a rectangular waveguide. So, scattering properties of the infinite PEC plane with a rectangular aperture and PEC plane with no apertures characterize the scattering parameters. In addition, propagation properties of free-space and rectangular waveguide characterize the propagation parameters of the system. Throughout the analysis only electric field interactions are taken in consideration and it is assumed that there is only TE_{10} mode inside the rectangular waveguide.

After obtaining the scattering and propagation supermatrices, system is reconstructed by BLT equation and all incoming and outgoing waves at the junctions are calculated. Since interiors of the shielding boxes are modeled as a tube with waveguide characteristics, electric field distribution at the center of the boxes is calculated by adding up two

outgoing waves form both ends and incoming to the center point. Note that the results of EMT method are in frequency domain and give information about change in the SE with respect to the frequency.

After obtaining the SE results by EMT method, they are compared with the CST MICROWAVE STUDIO® simulation results. When the results are compared, it is seen that they are very close to each other. SE of the boxes dramatically decreases at some resonant frequencies. It means that at those frequencies, shielding box cannot shield the device it enclosures. The information of resonant frequencies that SE decreases to a critical level is important and enough in some cases for the design of shielding boxes. Comparison of the results of EMT method and CST MICROWAVE STUDIO® simulation validates the accuracy of the EMT results, since they are very close to each other.

Additionally, response time of EMT method is very short. It solves the electromagnetic waves at every junction in only 5 seconds for our examples. On the other hand, CST MICROWAVE STUDIO® simulations take more than 300 seconds for same boxes. The analysis speed of the EMT method based on BLT equation will be more important for more complex systems. It simplifies the complex systems by modeling them as multiconductor transmission line networks and analyzes the waves at every point on the system very fast.

In conclusion, rectangular shielding boxes with one rectangular aperture are analyzed it this thesis by EMT method based on BLT equation with new modeling approach and assumptions and compared with the CST MICROWAVE STUDIO® simulation results. It is seen that EMT method provides a simple, fast and accurate technique to analyze the SE of shielding boxes.

In the future, this modeling approaches and assumptions can be improved using EMT method for multi-aperture shielding boxes with various aperture shapes, sizes and positions. In this thesis, shielding boxes are taken as there are no other elements in them that may cause extra reflections. As a future research activity, several electrical units can be put into shielding boxes such as printed circuit boards, cables, and etc. Then, these electrical units and equipments can also be modeled in the topological diagram of the system and their scattering and propagating characteristics can be used as a parameter in BLT equation. When it is achieved, a general insight of shielding box design will be obtained by a simple way and in a shortest time. Besides, an insight for the placement of the electrical units inside the shielding boxes will also be also acquired. This is also critical information for also Tempest applications. By this way, locations of the computers and other devices that emit EMR can be determined.

In addition, modeling of the topological diagram can be changed and used for an inverse problem. In other words, it can be assumed that EM source is inside the shielding box and EM field radiation from the apertures can be calculated. Application of the EMT method on such a problem will be very useful for both EMI problems and Tempest applications.

REFERENCES

[1] Y.-M. Park, Y. Lee, Y.-S. Chung, C. Cheon, and H.-K. Jung, "Electromagnetic Field Penetration Analysis of a Rectangular Aperture-Backed Cavity Based on Combination of Electromagnetic Topology and Mode Matching," *Electromagnetics*, vol. 29, no. 6, pp. 447–462, Aug. 2009.

[2] R. D. Leach and M. B. Alexander, "Electronic systems failures and anomalies attributed to electromagnetic interference," *NASA STI/Recon Technical Report*, 1995.

[3] C. Erbas and S. Kent, "Shielding effectiveness of a rectangular cavity with aperture between 1-3 GHz," *IEEE International Symposium of Electromagnetic Compatibility,* pp. 343–346, 2003.

[4] H. Mendez, "Shielding theory of enclosures with apertures," *IEEE TRANSACTIONS ON ELECTROMAGNETIC COMPATIBILITY*, vol. EMC-20, no. 2, pp. 296–305, 1978.

[5] M. D. Deshpande, "Electromagnetic Field Penetration Studies," no. June, 2000.

[6] M. Li, J. Nuebel, and J. Drewniak, "EMI from cavity modes of shielding enclosures-FDTD modeling and measurements," *IEEE Transactions on Electromagnetic Compatibility*, vol. 42, no. 1, pp. 29–38, 2000.

[7] G. Cerri, R. D. Leo, and V. M. Primiani, "Theoretical and Experimental Evaluation of the Electromagnetic Radiation From Apertures in Shielded Enclosures," *IEEE TRANSACTIONS ON ELECTROMAGNETIC COMPATIBILITY*, vol. 34, no. 4, pp. 423–432, 1992.

[8] J.-M. Jin and J. L. Volakis, "A finite-element-boundary integral formulation for scattering by three-dimensional cavity-backed apertures," *IEEE Transactions on Antennas and Propagation*, vol. 39, no. 1, pp. 97–104, 1991.

[9] C. H. Kraft, "Modeling Leakage Through Finite Apertures with TLM," 2000.

[10] M. Robinson, T. M. Benson, C. Christopoulos, J. F. Dawson, M. D. Ganley, A. C. Marvin, S. J. Porter, and D. W. P. Thomas, "Analytical formulation for the shielding effectiveness of enclosures with apertures," *IEEE TRANSACTIONS ON ELECTROMAGNETIC COMPATIBILITY*, vol. 40, no. 3, pp. 240–248, 1998.

[11] F. Po'ad and M. Jenu, "Shielding effectiveness of rectangular metallic enclosures with apertures," *ASIA-PACIFIC CONFERENCE ON APPLIED ELECTROMAGNETICS PROCEEDINGS*, pp. 167–171, 2005.

[12] Y.M. Park, Y. Lee, Y.S. Chung, C. Cheon, and H.-K. Jung, "Analysis of Electromagnetic Field Penetration Through Apertures Based on Electromagnetic Topology," *IEEE Antennas and Propagation Society International Symposium* , vol. d, no. 1, pp. 3–6, 2008.

[13] F. Tesche, "Topological concepts for internal EMP interaction," *IEEE Transactions on Antennas and Propagation*, vol. 26, no. 1, pp. 60–64, Jan. 1978.

[14] C. E. Baum, "The Theory of Electromagnetic Interference Control," *Interaction Notes-Note 597*, pp. 1–15, 1989.

[15] C. E. Baum, T. K. Liu, and F. M. Tesche, "On the analysis of General Multiconductor Transimission-Line Networks," *Interaction Notes-Note 350*, pp. 1–102, 1978.

[16] S. Celozzi, R. Araneo, and G. Lovat, *Electromagnetic Shielding*. Hoboken,New Jersey: Wiley-IEEE Press, 2008.

[17] Y. Park, Y. Lee, J. So, C. Cheon, Y. Chung, and H. Jung, "Electromagnetic Topology Combined with Mode Matching for the Electromagnetic Field Penetration Analysis of an Aperture Backed Cavity," pp. 121–126, 2009.

[18] T. T. Crow, Y. P. Liu, and C. D. Taylor, "Penetration of Electromagnetic Fields Through a Small Aperture into a Cavity," *Interaction Notes-Note 40*, pp. 1–10, 1968.

[19] Q. Liu, W. Yin, J. Mao, and Q. Liu, "Shielding effectiveness characterization of metallic enclosures with a thin-sheet panel illuminated by a arbitrary polarizations high-power EMP," *Asia-Pacific Symposium on Electromagnetic Compatibility and 19th International Zurich Symposium on Electromagnetic Compatibility* , no. May, pp. 19–22, 2008.

[20] G. Cerri and R. D. Leo, "Field penetration into metallic enclosures through slots excited by ESD," *IEEE TRANSACTIONS ON ELECTROMAGNETIC COMPATIBILITY*, vol. 36, no. 2, pp. 110–116, 1994.

[21] S. Sapuan and M. M. Jenu, "Shielding effectiveness and S21 of a rectangular enclosure with aperture and wire penetration," *Applied Electromagnetics,* pp. 1–5, 2007.

[22] M. Khorrami, P. Dehkhoda, R. Moini, and S. H. H. Sadeghi, "A fast shielding effectiveness calculation of rectangular enclosures with arbitrary shape apertures," *ASIA-PACIFIC CONFERENCE ON APPLIED ELECTROMAGNETICS PROCEEDINGS*, pp. 1–4, 2007.

[23] M. Robinson and J. Turner, "Shielding effectiveness of a rectangular enclosure with a rectangular aperture," *Electronics Letters*, vol. 32, no. 17, pp. 1559–1560, 1996.

[24] H. Bethe, "Theory of diffraction by small holes," *Physical Review Second Series*, vol. 66, pp. 163–182, 1944.

[25] H. W. Ott, *Noise reduction techniques in electronic systems*, 2nd ed. New York: Wiley, 1988.

[26] F. M. Tesche and C. M. Butler, "On the Addition of EM Field Propagation and Coupling Effects in the BLT Equation," *Interaction Notes-Note 588*, pp. 1–43, 2004.

[27] J. P. Parmantier, "An efficient technique to calculate ideal junction scattering parameters in multiconductor transmission line networks," *Interaction Notes-Note 536*, pp. 1–13, 1998.

[28] D. Pozar, *Microwave engineering*, Third Edit. Wiley, 2005, pp. 106–110.

[29] C. A. Balanis, *Antenna Theory*, Third Edit. Wiley, 2005, pp. 672–673.